PHYSICAL REVIEW B **76**, 140302(R) (2007)

Subdiffractive propagation of ultrasound in sonic crystals

Víctor Espinosa,[1] Víctor J. Sánchez-Morcillo,[1] Kestutis Staliunas,[2] Isabel Pérez-Arjona,[1] and Javier Redondo[1]
[1]*Departamento de Física Aplicada, Escuela Politécnica Superior de Gandia, Universidad Politécnica de Valencia, Crta. Natzaret-Oliva s/n, 46730 Grau de Gandia, Spain*
[2]*ICREA, Departament de Fisica i Enginyeria Nuclear, Universitat Politècnica de Catalunya, Colom 11, E-08222 Terrassa, Barcelona, Spain*

(Received 23 July 2007; published 31 October 2007)

We present an experimental demonstration of the subdiffractive propagation (self-collimation) of an ultrasound beam in a two-dimensional sonic crystal formed by a square array of steel cylinders inmersed in water. Measurements show that the diffractive spreading of a narrow beam is strongly reduced along the spatially modulated direction of the crystal. The effect of the finite crystal length is theoretically analyzed, resulting in a frequency shift of the subdiffractive point in good correspondence with the experimental results.

DOI: 10.1103/PhysRevB.76.140302 PACS number(s): 63.20.−e, 43.35.+d

The vanishing of diffraction or, in other terms, the self-collimation of wave beams, was predicted in the field of optics for electromagnetic waves propagating through optically periodic materials, the so-called photonic crystals.[1] Since its discovery, the phenomenon has attracted increasing attention and to date a number of applications for integrated optic devices have been proposed.[2] The phenomenon can be interpreted considering that the wave beam is composed by plane wave components (its spatial Fourier spectrum). The diffraction is then due to the dephasing of these plane wave components during propagation, which is ruled by the dispersion relation of the medium in which the beam propagates, $\omega(k_z,\mathbf{k}_\perp)$, with $\mathbf{k}_\perp=(k_x,k_y)$. The group velocity of each component is determined by the gradient of the frequency in k–space, $\mathbf{v}_g=\nabla_k\omega(\mathbf{k})$. As a consequence, for a given time- and space frequency component, the power propagates along the perpendicular direction of the spatial dispersion curves or equifrequency surfaces $k_z=f(\mathbf{k}_\perp)$. During a finite propagation distance l, the phase accumulated by any component is $\phi=k_z(\mathbf{k}_\perp)l$. In geometrical terms, the spatial dispersion curve is characterized by its curvature at each point, resulting in a corresponding diffractive broadening of the beam. As first pointed out in Ref. 1, in the case of photonic crystals, the isofrequency curves or surfaces two-dimensional [in (2D) or 3D structures, respectively] can develop flat segments at a particular frequency for a given geometry of the crystal. In this case, waves with wave vectors lying on the flat segment do not dephase during propagation through the crystal, and the beam propagates without apparent diffraction keeping its original size. This fascinating effect, originally named self-collimation, has been experimentally demonstrated to date for different frequency ranges of electromagnetic waves, in particular in the optical[3] and microwave[4] regimes.

The discussed effect is, however, generic and extendable to different kinds of waves, not restricted to the electromagnetic ones. The vanishing of diffraction in matter waves has been predicted, resulting in subdiffractive solitons in Bose-Einstein condensates.[5] Also recently, the subdiffractive propagation of sonic waves was predicted in phononic (or sonic) crystals.[6] The phenomenon, although based on the same physical grounds of the wave dynamics, shows, however, specific features in different systems. In the particular case of acoustics, two material parameters (the density and the bulk modulus) vary periodically in space, in contrast to the one-parameter variation for electromagnetic and matter waves. Here we present, for the first time, the experimental demonstration of the vanishing of diffraction for a ultrasonic beam propagating through a periodic medium.

The sonic crystal used in the experiments consisted in a squared array of 20×20 steel cylinders, each with a radius $r=0.8$ mm. The lattice constant (minimum distance between the centers of the scatterers) was $a=5.25$ mm, corresponding to a filling fraction $f=\pi(r/a)^2=0.073$. The total length of the crystal was $l=10$ cm. The crystal was immersed in a plexiglass tank, with dimensions $25\times25\times50$ cm^3, filled with water, which acted as a host medium. An ultrasonic source with radius $R=1.25$ cm was placed close to one of the flat boundaries of the crystal (entrance plane), and the pressure distribution was measured with a needle hydrophone. The source radiates an ultrasonic beam with measurable amplitude in the frequency interval ranging from 150 to 260 KHz.[7] As will be discussed later, this suggests the experiments to be done in the second propagation band. All the signal generation and acquisition process is based on a National Instruments PXI-technology controller NI8176, which also controls an OWIS GmbH two-axis motorized system that allows the hydrophone to scan the pressure distribution at the plane transversal to the propagation for a given frequency component.

The experiment was designed based on the theoretical analysis and numerical simulation of the equation describing the propagation of sound waves in inhomogeneous media,

$$\frac{1}{\bar{B}(\mathbf{r})}\frac{\partial^2 p(\mathbf{r},\tau)}{\partial\tau^2}-\nabla\left[\frac{1}{\bar{\rho}(\mathbf{r})}\nabla p(\mathbf{r},\tau)\right]=0, \qquad (1)$$

where $p(\mathbf{r},\tau)$ is the scalar pressure field, $\bar{B}(\mathbf{r})=B(\mathbf{r})/B_h$ and $\bar{\rho}(\mathbf{r})=\rho(\mathbf{r})/\rho_h$ are the spatially dependent bulk modulus density, both normalized to the corresponding values in the host medium. A dimensionless time $\tau=c_h t$ is also defined, with $c_h=\sqrt{B_h/\rho_h}$. This time normalization makes the velocity of sound in the host medium equal to unity. The lattice is defined through the centers of the cylinders by the set $\mathcal{R}=\{\mathbf{R}=n_1a_1+n_2a_2;n_1,n_2\in N\}$ of two-dimensional lattice vectors

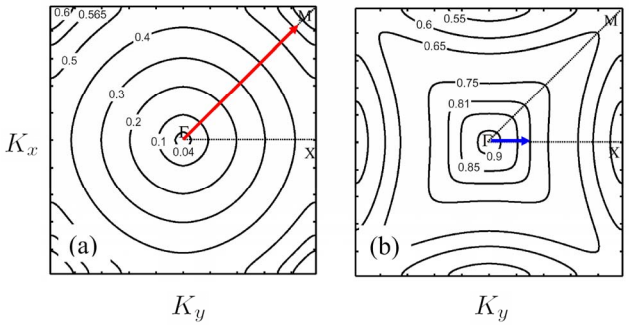

FIG. 1. (Color online) Isofrequency lines, evaluated for $a=5.25$ mm and $r=0.8$ mm, for the first (a) and second (b) bands, centered at the point Γ, using the plane wave expansion method. The axes have unit length (the first Brillouin zone is shown). Numerals denote the reduced frequency $\Omega=\omega a/2\pi c_h$. The arrows indicate the location of the flat regions, and consequently to wave vectors belonging to a self-collimated beam.

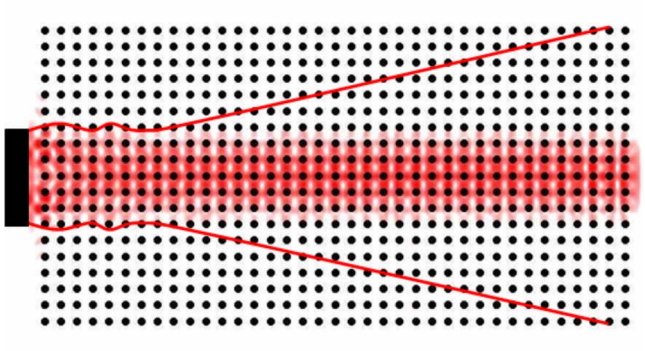

FIG. 2. (Color online) Numerical simulation of the propagation of an ultrasonic beam in a self-collimated mode in the second band. The lines represent the lobe of the beam propagating in a homogeneous medium. Source frequency is 230 KHz in both cases. The radius of the plane source is $R=1.25$ cm, and the crystal parameters as in Fig. 1.

R generated by the primitive translations a_1 and a_2. In our case, $a_1=a_2=5.25$ mm. The corresponding reciprocal lattice is defined through the set $\mathcal{G}=\{\mathbf{G}:\mathbf{G}\cdot\mathbf{R}=2\pi n; n\in N\}$. The material parameters are $\rho_h=10^3$ Kg m^{-3}, $B_h=2.2\times10^9$ N m^{-2} for water, and $\rho_s=7.8\times10^3$ Kg m^{-3}, $B_s=160\times10^9$ N m^{-2} for steel, resulting in the sound velocities $c_h=1483$ m s^{-1} and $c_s=4530$ m s^{-1}.

To determine theoretically the optimal conditions for the subdiffractive propagation of a sonic beam, we first calculated the families of the spatial dispersion curves and identified the frequencies corresponding to the flat regions (straight equifrequency lines in our 2D case). If we consider that the initial beam is monochromatic, $p(\mathbf{r},t)=p(\mathbf{r})e^{i\omega\tau}$, then one can substitute $\partial^2/\partial t^2\rightarrow-\omega^2$ and eliminate the temporal dependence from Eq. (1). The dispersion relation $\omega=\omega(\mathbf{k})$ has been computed using the plane wave expansion (PWE) method, where the pressure field as well as the material parameters (density and bulk modulus) are Fourier expanded on the basis of the reciprocal lattice, i.e. $p(\mathbf{r})=e^{i\mathbf{k}\cdot\mathbf{r}}\sum_{\mathbf{G}}p_{\mathbf{k},\mathbf{G}}e^{i\mathbf{G}\cdot\mathbf{r}}$ for the pressure, and analogously for the other magnitudes (see Ref. 6 for details). This expansion converts a differential equation (1) into an infinite matrix eigenvalue problem, to be truncated and solved numerically. By solving the eigenvalue problem one obtains the frequencies corresponding to each Bloch wave characterized by **k** (the two-dimensional Bloch vector restricted to the first Brillouin zone), resulting in the dispersion relation of the periodic medium. In Fig. 1 the isofrequency contours are plotted for the first [Fig. 1(a)] and second [Fig. 1(b)] propagation bands, for the parameters corresponding to our experimental setup.

The analysis of the families of isofrequency curves shows that there always exists a particular frequency corresponding to a flat segment, in each propagation band. The corresponding direction of the subdiffractively propagating waves in **k**-space depends on the number of the propagation band: e.g. at 45° with respect to the crystal axes, i.e. in the $\langle1,1\rangle$ direction, for the first band, or along the crystal axes, i.e. in the $\langle1,0\rangle$ and $\langle0,1\rangle$ directions, for the second band. The subdiffractive frequencies are slightly less than the frequencies of the upper edge of the corresponding bands [denoted by the points M and Γ in Figs. 1(a) and 1(b), respectively], by an amount proportional to the filling factor. The asymptotic analysis in the limit of small filling factor, discussed in detail in Ref. 6, leads to the relation $\omega_{nd}=\omega_g(1-f^{2/3})$, where ω_{nd} and ω_g are the angular frequencies corresponding to the zero diffraction and to the middle of the band gap, respectively. It is common to express the frequency and wave vector in terms of their reduced (adimensional) values, defined as $\Omega=\omega a/2\pi c_h$ and $\mathbf{K}=\mathbf{k}a/2\pi$; in this case the band-gap frequencies take the values $\Omega_g=1/\sqrt{2}$ and 1 for the first and second bands, respectively. The asymptotic analysis also allows us to evaluate the width of the flat segments, as $\Delta k_\perp=|\mathbf{K}_g|f^{2/3}$, where $|\mathbf{K}_g|=\Omega_g$. The width of the flat segments is inversely proportional to the minimum width of the subdiffractively propagating beams, and is a significant factor in seeking the experimental demonstration of the phenomenon.

The predictions of the previous analysis have been confirmed by the numerical simulation of Eq. (1) using the finite difference in time domain (FDTD) technique,[8] where an input beam with the above calculated subdiffractive frequency in the second band was propagated through the crystal. A typical result, obtained for medium parameters corresponding to our experimental setup and a source frequency of 230 KHz, close to the subdiffractive propagation frequency in the second band, is shown in Fig. 2, where the effect of self-collimation is convincing. For comparison, the size of a beam (its central lobe) of the same frequency propagating without crystal is shown by lines. The numerical analysis shows that the optimum collimation (that corresponding to a beam of the minimum width at the exit plane of the crystal) occurs at a frequency slightly less than that evaluated above. The interpretation for this "discrepancy" is given below.

The experimental evidence of ultrasound self-collimation was obtained by measuring the two-dimensional pressure distribution across the transverse plane of the beam in three situations, as shown in Fig. 3: in case (a) close to the source ($z=5$ mm), in case (b) at $z=105$ mm from the source in the absence of crystal, and in case (c) at the exit plane of the

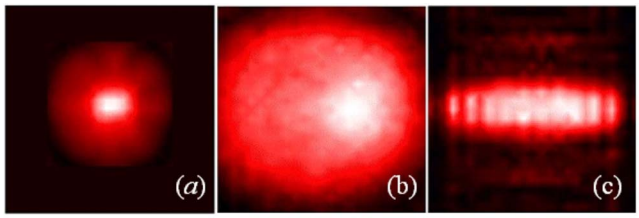

FIG. 3. (Color online) Transverse pressure distribution of the beam for 230 KHz. (a) at $z=5$ mm (near the source), (b) at $z=105$ mm propagating in water, and (c) at the same distance, after propagating through the crystal.

crystal, located at the same distance from the source as in case (b). The transverse plane was scanned in steps of 1 mm, and the resulting distribution was later interpolated in order to get the smooth distributions shown in Fig. 3. Figure 3(b) illustrates the expected diffractive broadening after propagation in a homogeneous medium. In this case the width of the beam is roughly determined by the number of Rayleigh lengths, $z_R=\omega R^2/2c_h$ the beam has propagated in the medium. For the considered case, $z_R\sim 7$ cm, which means that the propagation over the distance of $z=10$ cm should result in a beam size three times larger that of the input beam, which is in a good agreement with the measurements (see also Fig. 4). In the presence of the sonic crystal, the beam evolved into a elliptic one after the propagation [Fig. 3(c)]. In this case, the beam was strongly diffracted in the horizontal direction, i.e. along the direction of the steel cylinders, since in this direction any spatial modulation is absent. The diffraction in the vertical direction, where the modulation was present, was strongly suppressed, and the final width of the beam remains nearly the same as at the entrance.

The comparison between the experimental and theoretical results can also be shown by inspecting the 1D transverse cross section of the beam distribution, at the exit plane, with

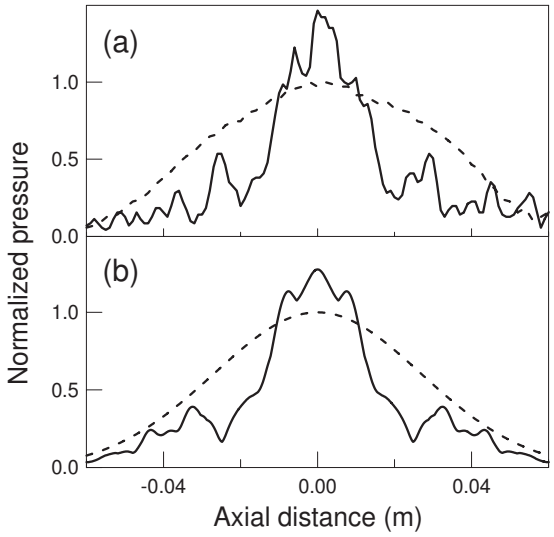

FIG. 4. Cross section of the beam at the exit plane of the crystal (continuous line), and at the same distance from the source without crystal (dashed line), as measured (a) and evaluated numerically (b). Parameters as in Fig. 3.

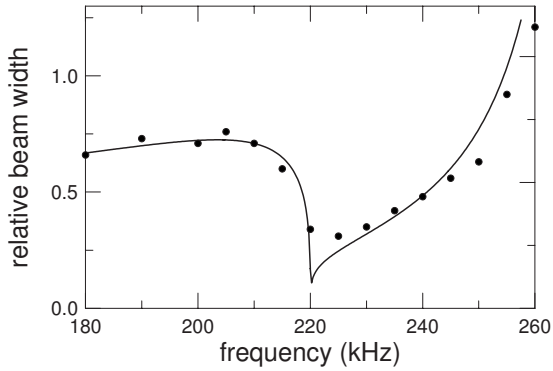

FIG. 5. Relative width depending on the frequency. The symbols correspond to experimental results, and the curves to the analytical expressions Eqs. (2) and (3) evaluated for $\delta=0.02$ rad and $l=0.1$ m.

and without crystal. Figure 4(a) shows the measured beam cross section at $x=0$ and $z=10$ cm from the source, both with (continuous line) and without (dashed line) the sonic crystal. Figure 4(b) shows the numerical results corresponding to the FDTD simulation of Eq. (1). The vertical axis corresponds, in both cases, to the pressure amplitude normalized to the maximum pressure in the case of free propagation.

Finally, we explored the dependence of the beam width on the frequency of the ultrasound in order to locate the optimum frequency for the self-collimation. The results are summarized in Fig. 5. The beam width has been evaluated at the exit plane as the corresponding to one half of the maximum pressure value. The resulting width has been normalized to the width of the beam after propagating the same distance from the source without crystal. In this way, the undesired effects of the frequency-dependent initial width, and the inhomogeneities in the initial distribution due to the excitation of different modes in the transducer, can be neglected. The experimental results are represented in Fig. 5 by symbols. It is clearly appreciated that the beam width presents a minimum at around 225 KHz. At this value, the beam width at the entrance and exit planes remains nearly the same (see also Fig. 4), evidencing the disappearance of diffraction.

The frequency for which the beam presents the minimum width, however, does not exactly coincide with the calculated zero-diffraction frequency (230 KHz), being slightly less. We interpret this discrepancy as a propagation-over-finite-distance effect. The spatial dispersion curve is never flat on an entire segment—the curvature can become zero just on one or several points on the smooth curve (more than two times differentiable function). Therefore the beam, even at the zero-diffraction point, weakly broadens in the propagation. This subdiffractive broadening at the zero-diffraction point (corresponding to $\partial^2 k_\parallel/\partial^2 k_\perp=0$) is determined by the higher order spatial derivatives, and in particular by the fourth order derivative is this symmetric case $\partial^4 k_\parallel/\partial^4 k_\perp$.[5] In this way the spatial dispersion curve can be expanded as $k_\parallel(k_\perp)=k_{\parallel,0}+d_2k_\perp^2+d_4k_\perp^4$, with diffraction coefficients $d_2\propto 1-f^2/\Delta\omega^3$, $d_4\propto 1/\Delta\omega^2-f^2/\Delta\omega^5+1/4-f^2/\Delta\omega^4$, where $\Delta\omega=(\omega_g-\omega)/\omega_g$, as follows extending the asymptotic analysis in Ref. 6. At the zero-diffraction point ($\Delta\omega=f^{2/3}$) then $d_4\propto 1/4-f^{-2/3}$. To calculate the minimum width of the subdif-

fractively propagating beam over a finite distance l, the dephasing of the corresponding components of the beam should be insensible over that distance: $|\Delta k_{\|}|l=\delta \ll 1$, where $|\Delta k_{\|}|$ is the variation of the longitudinal component of the wave vector "over the beam." Given the dispersion relation $k_{\|}(k_{\perp})$, the corresponding width of the beam can be determined for a finite propagation distance. A simple analysis of the above fourth-order expansion of dispersion relation yields that negative values of d_2 (the region of the slightly positive diffraction of the leading order since $d_2<0$ corresponds to normal diffraction) is optimal. In particular, the optimum self-collimation occurs at $d_2=d_2^0=-2\sqrt{d_4\delta/l}$, which corresponds to the maximum width of the spatial spectra $k_{\perp}^2 \approx -d_2/d_4$, or the minimum width of the beam $x_0 \approx k_{\perp}^{-1}$.

In Fig. 5 the width of the beam at the exit plane of the crystal is given depending on the frequency, as measured experimentally (symbols) and as evaluated analytically following the above discussion (solid lines). The analytic curve is discontinuous, i.e consisting of two branches,

$$k_{\perp}^2 \approx -d_2/2d_4 + \sqrt{\delta/(ld_4)} \tag{2}$$

for $d_2>d_2^0$, and

$$k_{\perp}^2 \approx -d_2/2d_4 - \sqrt{(d_2/2d_4)^2 - \delta/(ld_4)} \tag{3}$$

for $d_2<d_2^0$.

The left and right branches in Fig. 5 correspond to a normalized width $x/x_0=(x_0k_{\perp})^{-1}$, with $k_{\perp}$ given by Eqs. (2) and (3), respectively. Both the phase δ and the normalization factors x_0 have been chosen to get the best fit to the experimental data. The experimental points fit well to the theoretical curve away from the discontinuity, but cannot follow precisely the sharp break at the discontinuity. The pressure distribution in the beam is also in accordance with the above analysis. The beams present a relatively smooth envelope at frequencies larger than critical ($d_2>d_2^0$), because the dispersion curve shows a single minimum, and present pronounced oscillatory fronts for smaller frequencies ($d_2<d_2^0$), as the dispersion curve shows double minima. This is the case shown in Fig. 4. Simply speaking, the flat segment is broader in the case when it is almost flat, but with a weak bump in the middle, than a perfectly flat one.

In conclusion, the subdiffractive propagation of ultrasonic beams in a 2D sonic crystal has been demonstrated experimentally. Such materials have recently attracted great interest,[9] because of their potential applications in the control of sound propagation, used as reflectors, focusers,[10] or waveguides.[11] Such subdiffractive sonic beams are supported by crystals with perfect symmetry, and do not require the presence of defects, different from other waveguiding phenomena previously reported.[11] The phenomenon is independent of the spatial scale and consequently it must be observable in other (e.g. audible) regimes, as well as in the 3D case.

The work was financially supported by the Spanish Ministerio de Educación y Ciencia and the European Union FEDER (Projects Nos. FIS2005-07931-C03-02 and -03, and Programa Juan de la Cierva). K.S. has been partially supported by a grant of the Politechnical University of Valencia.

[1] H. Kosaka, T. Kawashima, A. Tomita, M. Notomi, T. Tamamura, T. Sato, and S. Kawakami, Appl. Phys. Lett. **74**, 1212 (1999).

[2] D. W. Prather, S. Shi, J. M. Murakowski, G. J. Schneider, A. Sharkawy, C. Chen, B. Miao, and R. Martin, J. Phys. D **40**, 2635 (2007).

[3] P. T. Rakich, M. S. Dahlem, S. Tandon, M. Ibanescu, M. Soljai, G. S. Petrich, J. D. Joannopoulos, L. A. Kolodziejski, and E. P. Ippen, Nat. Mater. **5**, 93 (2006).

[4] Z. Lu, S. Shi, J. A. Murakowski, G. J. Schneider, C. A. Schuetz, and D. W. Prather, Phys. Rev. Lett. **96**, 173902 (2006).

[5] K. Staliunas, R. Herrero, and G. J. de Valcárcel, Phys. Rev. E **73**, 065603(R) (2006).

[6] I. Pérez-Arjona, V. J. Sánchez-Morcillo, J. Redondo, V. Espinosa, and K. Staliunas, Phys. Rev. B **75**, 014304 (2007).

[7] The emitting broadband transducer had a resonant frequency of 192 KHz, corresponding to its maximum efficiency. The measured signal was filtered, the receiver hydrophone being sensitive to a central frequency, coincident to the excitation frequency, and to those lying in a bandwidth of 10% around that central frequency.

[8] J. O. Vasseur, B. Djafari-Rouhani, L. Dobrzy'nski, M. M. Kushwaha, and P. Halevi, J. Phys.: Condens. Matter **6**, 8759 (1994).

[9] J. H. Page, A. Sukhovich, S. Yang, M. L. Cowan, F. Van der Viest, A. Tourin, M. Fink, Z. Liu, C. T. Chan, and P. Sheng, Phys. Status Solidi B **241**, 3454 (2004).

[10] S. Yang, J. H. Page, Z. Liu, M. L. Cowan, C. T. Chan, and P. Sheng, Phys. Rev. Lett. **93**, 024301 (2004); M. Torres and F. R. Montero de Espinosa, Ultrasonics, **42**, 787 (2004).

[11] T. Miyashita, Meas. Sci. Technol. **16**, R47 (2005).